

First Principles Investigation of FeCo Alloy: Electronic and Optical Properties Study

Ali Hossain^{1, 2, *}, Rafiqul Islam³

¹Department of Chemical Nanoengineering, University of Aix-Marseille, Marseille, France

²Department of Physics, University of Rajshahi, Rajshahi, Bangladesh

³Department of Electrical & Electronic Engineering, Manarat International University, Dhaka, Bangladesh

Email address:

haliru10@gmail.com (A. Hossain), rafiq.amath@gmail.com (R. Islam)

*Corresponding author

To cite this article:

Ali Hossain, Rafiqul Islam. First Principles Investigation of FeCo Alloy: Electronic and Optical Properties Study. *Engineering Physics*. Vol. 3, No. 1, 2019, pp. 1-5. doi: 10.11648/j.ep.20190301.11

Received: October 21, 2018; **Accepted:** January 14, 2019; **Published:** January 31, 2019

Abstract: The ground state electronic structures and optical properties of FeCo alloy have been reported using plane wave ultrasoft pseudopotential based on spin polarized density functional theory through first principles study. The crystallographic structure of FeCo consists with body-centered cubic lattice that is described in space group $Im-3m$ (229). The geometry is optimized with zero applied pressure and the optimized lattice constant is found to be 2.854\AA . The electronic energy bands represent the overlapped between valence and conductance electronic states and confirm zero forbidden gaps i.e. metallic nature of the FeCo alloy. The Fermi surfaces manifest the anisotropic features of electronic energy dispersion along the high symmetry directions (X-R-M-G-R) of the Brillouin zone. The total density of states arises from the contribution of the electronic states of Co and Fe atoms. The calculated spin magnetic moments of FeCo alloy is $1.26\mu_B$. The spin magnetic moments mainly come from the exchange interactions among electronic spins, which confirms the strong electron-electron interactions. Moreover, the optical properties are computed which also attest the metallic behavior of the material. The optical measurements indicate that FeCo alloy is an optically anisotropic material. The obtained loss spectrum reveals the plasmonic excitations that is important for many magneto-optical applications.

Keywords: FeCo, Spin Polarization, Magnetic Moments, Optical Properties, Plasmon

1. Introduction

The ferromagnetic bimetallic alloys have flourished as materials of extensive importance and many scopes in different fields of materials science and engineering. Only Fe, Co, Ni and their alloys (FeCo, CoNi and FeNi) shows ferromagnetic behavior at room temperature [1]. Among them, FeCo has greater attraction due to its unique physical and chemical properties. Such as large value of saturation magnetization, high permeability, low coercivity, high curie temperature, low dielectric constant, excellent chemical stability and mechanical hardness, etc. For these properties, it is suitable for various chemical technological applications for instance, transformer core, electric motor, pole pieces, high temperature magnet, biomedicine, magnetic resonance imaging, hyperthermia-based therapy and specially data

storage and so on. [2-9]

Many density functional studies have been performed on FeCo using first principles through various approximations such as coherent potential approximation (CPA) and local spin density approximation (LSDA) [9-10]. In this study, spin polarized density functional theory (DFT) have been applied through generalized gradient approximation (GGA) approached to obtain the electronic structures and optical properties of FeCo alloy. The optical properties of FeCo alloy based on spin polarized DFT are rarely reported. The investigation with considering electronic spin has great importance for FeCo alloy to search its applicability in field of spintronics. The electronic band structures, density of states and optical properties such as dielectric function, absorption, refractive index, loss spectra and optical reflectivity have been computed. This study manifests the significance of electronic spin polarization and the picture of

electronic spin interactions. Moreover, the study of optical loss function as well as plasmonic excitations have been carried out that is expected for magneto-optical applications.

2. Computational Modelling

Based on density functional theory (DFT), the electronic structure calculation and structure optimization of FeCo alloy was performed by using first principles employed in CASTEP code [11]. The energy cut-off and number of k-points that measures how well one discrete grid has appointed the continuous integral have been used. The treated valence electron configurations are $3d^6 4s^2$ for Fe and $3d^7 4s^2$ for Co respectively. The interactions among valence electrons and ions are considered using the Vanderbilt type ultrasoft pseudopotential (UPP) formalism [12-14]. UPPs attain much softer pseudo-wave function that considerably used fewer plane waves for calculations of the same accuracy. The Broyden-Fletcher-Goldfarb-Shanno (BFGS) minimization techniques have been utilized to obtain the ground state energy configuration of the FeCo alloy [15].

The optimizations were performed through plane wave energy cut-off of 1200 eV and $22 \times 22 \times 22$ Monkhorst-Pack [16] grid parameter for sampling of the Brillouin zone for FeCo alloy. The GGA of the Perdew-Burke-Ernzerhof (PBE) formalism is used to evaluate the exchange-correlation energy [17]. Optimization is operated using convergence thresholds of 10^{-5} eV/atom for the total energy and 10^{-3} Å for maximum displacement. Maximum force and stress are 0.03 eV/Å and 0.05 GPa respectively for all the calculations.

The optical properties of FeCo alloy can be described entirely by complex dielectric function $\epsilon(\omega) = \epsilon_1(\omega) + i\epsilon_2(\omega)$, which correlated with interactions of photons and electrons at all frequencies. The imaginary part $\epsilon_2(\omega)$ of dielectric function from the momentum matrix elements between the occupied and unoccupied wave functions, which is given by,

$$\epsilon_2(\omega) = \left(\frac{4\pi^2 e^2}{m^2 \omega^2} \right) \sum_{i,j} \int \langle i | M_d | j \rangle^2 f_i (1 - f_j) \delta(E_f - E_i - \omega) d^3 k \quad (1)$$

where, M_d is the dipole matrix, i and j are the initial and final states respectively, f_i is the Fermi distribution function for the i -th state, and E_i is the energy of electron in the i -th state. The real part $\epsilon_1(\omega)$ of dielectric function can be evaluated from $\epsilon_2(\omega)$ using Kramers-Kronig relations [18] as follows

$$\epsilon_1(\omega) = 1 + \frac{2}{\pi} P \int_0^{\infty} \frac{\omega' \epsilon_2(\omega') d\omega'}{(\omega'^2 - \omega^2)} \quad (2)$$

where, P implies the principal value of the integral. The knowledge of both the real and imaginary parts of the dielectric tensor allows the calculation of important optical functions. The dielectric function, the optical reflectivity, the absorption coefficient, the electron energy loss spectrum as well as the refractive index (n) and the extinction coefficient (k) have been computed.

3. Results and Discussions

3.1. Crystallographic Structure of FeCo

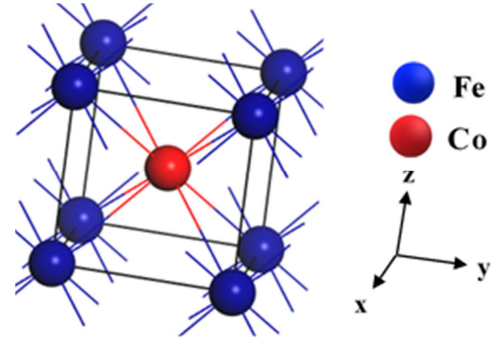


Figure 1. The crystallographic structure of FeCo alloy.

The FeCo structure is based on body-centered cubic lattice that is described in the space group $Im-3m$ (229). The geometry optimization is performed with zero applied pressure to investigate the structural properties of ground state configuration of FeCo alloy. Then the optimized unit cell, lattice parameter and equilibrium volume also obtained from this simulation. The crystallographic structural unit cell of FeCo consists of one formula unit. The Fe and Co atoms occupied in Wyckoff positions 2a (0, 0, 0) and 2a (1/2, 1/2, 1/2) respectively, in the lattice sites. Figure 1 shows the crystal structure of FeCo in which the Fe atoms occupied primitive cubic sites and Co atom appears at the center of the unit cell. The optimized value of the lattice parameter is found to be 2.854 Å that is consistent with reported experimental values [4, 6, 9].

3.2. Electronic Properties

3.2.1. Structure of Energy Bands

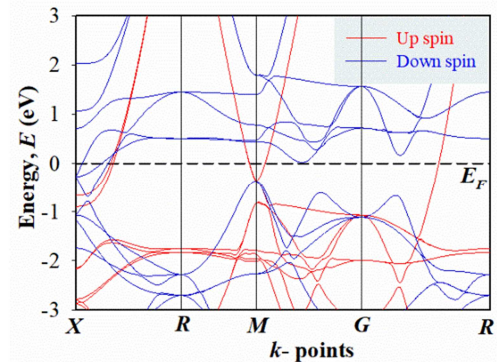


Figure 2. The energy bands of FeCo along the high symmetry directions (X-R-M-G-R) of the Brillouin zone.

The electronic band structures have been computed to understand the shape of the valence and conduction bands. The properties of the material can be understood by identifying the character of dominant bands near the Fermi level, their energy etc. The energy bands of FeCo is shown in Figure 2 at zero pressure along the high symmetry directions (X-R-M-G-R) of the Brillouin zone in the energy range from

-3 to +3 eV. The Fermi level is chosen to be the zero of the energy scales. The valence and conduction bands of FeCo are seen to overlap, thus indicating metallic-like behavior of the alloy. In addition, the band structure also shows strongly anisotropic features with characteristics energy dispersion along the axial axes, such as X-R and M-G directions. Consequently, the electrical conductivity is anisotropic for FeCo alloy, i.e., the electrical conductivity possesses different values for each crystal plane.

3.2.2. Density of States (DOS) and Spin Magnetic Moments.

The DOS determines the number of electronic states per unit energy. The Fermi level position is taken as reference point for determining DOS. The DOS of FeCo is shown in Figure 3. It is seen from Figure 3, that the TDOS reveals non-zero values at Fermi level, E_F . These non-zero values of total DOS (TDOS) manifest the metallic nature of FeCo with the evidence of zero energy gaps, which also attests the energy band diagram as shown in Fig. 2 [9].

At the Fermi energy, E_F , the values of TDOS and spin DOS (SDOS) are 1.94 and 1.26 states/eV per unit cell, respectively. The values of SDOS at Fermi level arise due to polarizations of the spin states, which are.

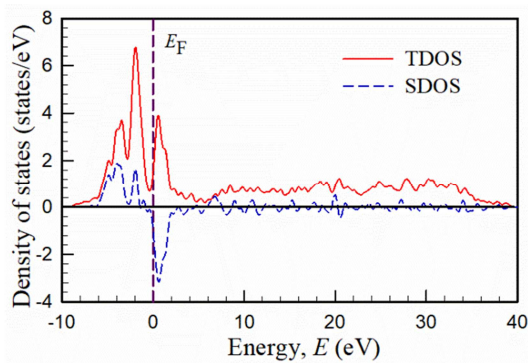


Figure 3. TDOS & SDOS of FeCo as a function of energy in eV.

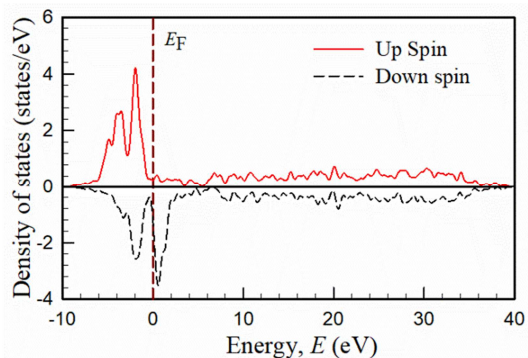


Figure 4. DOS from up spin and down spin electronic states of FeCo as a function of energy in eV.

Expected for this type of bimetallic alloy. The spin polarizations manifest the exchange interactions of electronic energy states and confirms strong electron-electron interactions. The dissimilarities between up spin and down spin confirm the spin polarization states for FeCo as shown in Figure 4.

The calculated total spin magnetic moments is found to be $1.26\mu_B$ that due to the consequence of strong electron-electron interactions. The higher values of DOS below the Fermi level manifests the hybridization 3d electronic states of Fe and Co atoms, which are also seen from Figure 5 & Figure 6. The projected DOS (PDOS) determine the occupied electronic states per unit energy contributing from individual atoms. The Fe 3d electrons provide PDOS and SDOS are 0.83 and 0.71 states/eV, respectively, at Fermi level as presented in Figure 5. In addition, it is seen from Figure 6 that the values of PDOS and SDOS at Fermi level are 0.48 and 0.37 states/eV, respectively per unit cell due to Co 3d electrons.

The values of SDOS of Fe and Co atoms yield the spin polarization that is induced due to presence of spontaneous spin magnetic moments of the atoms. The calculated spin magnetic moments for Fe and Co atoms are found to be $0.85\mu_B$ and $0.41\mu_B$, respectively. The calculated spin magnetic moments are slightly smaller than the reported values [9, 11]. The results are consistent, but small variations appeared due to different atomic occupancies and compositions.

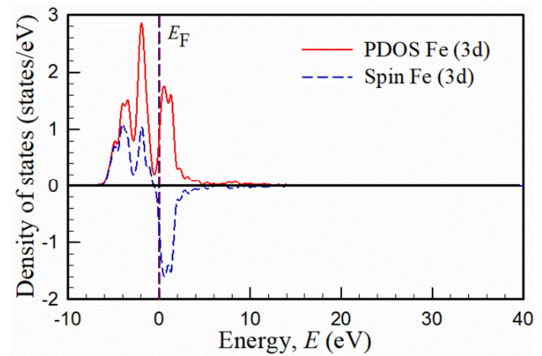


Figure 5. Projected DOS of Fe (3d) atoms as a function of energy in eV.

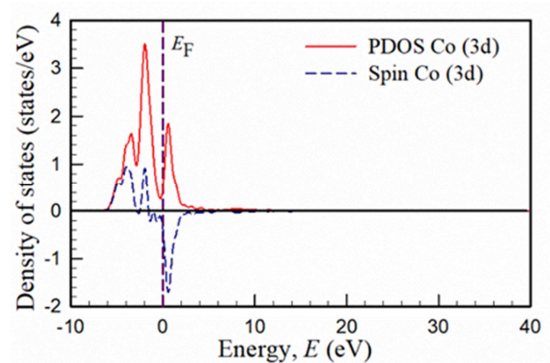


Figure 6. Projected DOS of Co (3d) atoms as a function of energy in eV.

3.3. Optical Properties

The optical properties of FeCo alloy have been analyzed as a function of incident photon energies for [100] crystallographic polarization direction up to 50 eV. A Drude term with unscreened plasma frequency 3 eV and damping 0.05 eV has been used to enhance the low energy part of the spectrum. The optical properties are much correlated with

each other. Such as where the lowest value of real part of dielectric function appear, that correspond to the first peak in reflectivity and absorption spectra. The dielectric function explains how a material response to the electromagnetic radiation, in particular to visible light.

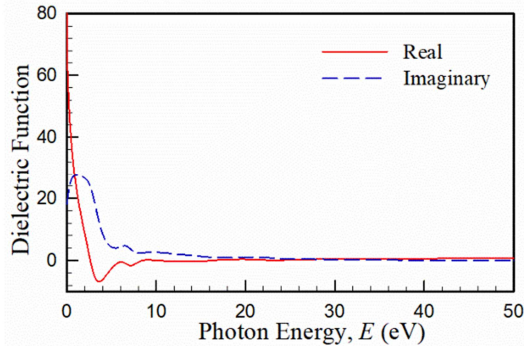


Figure 7. Dielectric function of FeCo alloy with incident photon energy, E (eV).

Both the real and imaginary part of dielectric function indicates the metallic characteristics of the material. For the metallic compounds both inter-band and intra-band transitions contribute to dielectric functions. It is seen from Figure 7 that the real part of dielectric function exhibits characteristic peak at 3.6 eV. The negative value of the real part of dielectric function indicates that the FeCo shows the intraband Drude-like behavior. At high energy region, the dielectric function tends to zero. It manifests itself as almost transparent material that means the material is optically anisotropic. Therefore, the dielectric formalism mainly arises from electronic polarizability, since at high energy region the effect of ionic and dipolar polarizability is negligible. The absorption spectrum shows in Figure 8 some characteristics peaks that reveal due to electronic transition of Co/Fe from p to d states.

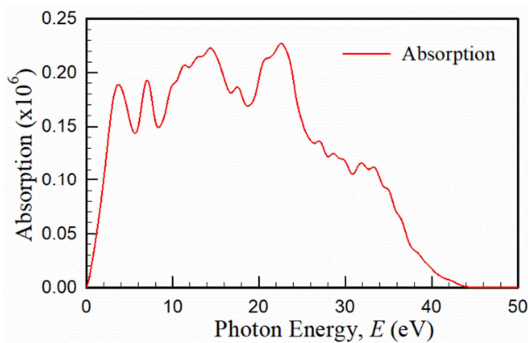


Figure 8. Absorption of FeCo alloy with incident photon energy, E (eV).

The simulated result of the refractive index of FeCo is presented in Figure 9. The real part of refractive index determines the phase velocity and the imaginary part determines the amount of absorption loss when an electromagnetic wave passes through the materials. It is seen in figure, that the real part of refractive index, n sharply decreased in low energy region up to 4.8 eV and then it is

almost constant up to 50 eV. Moreover, extinction coefficient, k linearly increases up to 3.5 eV and then decreases almost exponentially that indicates how incident energy absorbed in the materials. The computed energy loss spectra are shown in Figure 10. The energy loss function of materials is very important parameter in the dielectric formalism, which is useful to understand the screened excitation spectra, especially the collective excitations produced by the swift charges

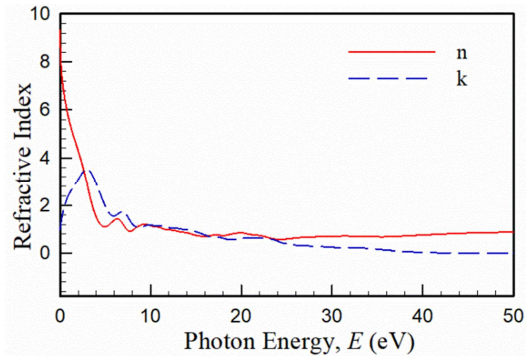


Figure 9. Refractive index of FeCo alloy with incident photon energy, E (eV).

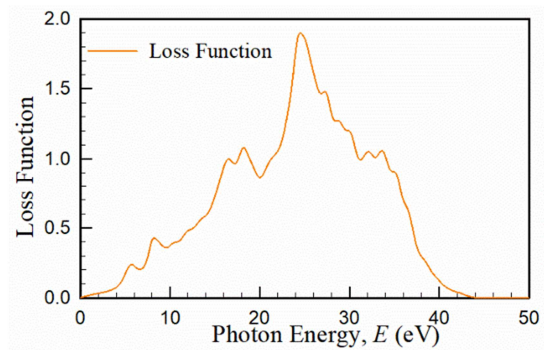


Figure 10. Loss function spectra of FeCo alloy with incident photon energy, E (eV).

Inside a solid. Loss function refers to the fast electron traversing in a material. The highest peak of the energy loss spectrum appears due to bulk plasmonic excitation at particular incident photon energy as well as the corresponding frequency known as the bulk plasma frequency. In loss spectrum, the plasma frequency is located at 24.52 eV. The other characteristics peaks reveal surface plasmonic excitations due to optical transition instead of absorbing high energy photons. This type of loss spectroscopy predicted that the compound is applicable for guiding of light below the diffraction limit (near-field optics), non-linear optics, bio-sensors etc. [19]. Moreover, the peaks of loss spectrum indicate the large magneto-optical Kerr effect (MOKE) which is expected for high density storage media [20]. The calculated optical reflectivity anomalously decreases with increasing incident photon energy as presented in Figure 11.

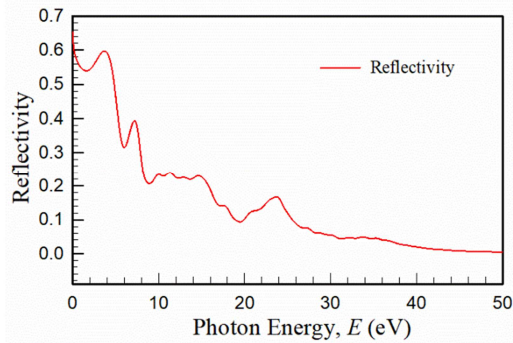


Figure 11. Reflectivity of FeCo alloy with incident photon energy, E (eV).

4. Conclusions

The ground state electronic and optical properties of FeCo alloy through density functional theory by employing ultrasoft pseudopotential is reported. The computational electronic structure analysis confirms no band gaps at Fermi level and the metallic nature of the material. The energy dispersion along the Fermi level manifest the electronically anisotropic features of the FeCo alloy. The density of states reveals that the electronic properties of FeCo are mainly attained from the contribution of 3d electronic states of Fe and Co atoms. The electronic spins split energy states and the high spin magnetic moments found due to strong electron-electron interactions. The calculated spin magnetic moment is found to be $1.26\mu_B$. Thus, FeCo alloy may be used for spintronics applications. In addition, the optical measurements show that FeCo alloy is an optically anisotropic material. The loss spectroscopy indicates the plasmonic excitations that is important for many magneto-optical applications.

Acknowledgements

The authors would like to acknowledge Materials Science Laboratory, Department of Physics, University of Rajshahi, Bangladesh for technical supports related to this work.

References

- [1] N. Spaldin, *Magnetic Materials*, Cambridge University Press, Cambridge, (2003).
- [2] C. Kumar, F. Mohammad (2011), *Magnetic Nanomaterials for Hyperthermia-Based Therapy and controlled Drug Delivery*. *Adv. Drug Deliv. Rev.* 63, 789-808.
- [3] A. H. Habib, C. L. Ondeck, P. Chaudhary, M. R. Bockstaller and M. E. McHenry (2008), Evaluation of Iron-Cobalt/Ferrite Core Shell Nanoparticles for Cancer Thermo-therapy. *J. Appl. Phys.* 103, 07A307:1-4.
- [4] E. Thirumal, D. Prabhu, K. Chattopadhyay and V. Ravichandran (2010), Magnetic, Electric, and Dielectric Properties of FeCo Alloy Nanoparticles Dispersed in Amorphous Matrix. *Phys. Status Solidi A* 207, 2505-2510.
- [5] A. Shokuhfar and S. S. S. Afghahi (2013) The heating effect of iron-cobalt magnetic nanofluids in an alternating magnetic field: application in magnetic hyperthermia treatment, *Nanoscale Research Letters* 8, 540:1-11.
- [6] S. J. Lee, J. H. Cho, C. Lee, J. Cho, Y. R. Kim and J. K. Park (2011) Synthesis of Highly Magnetic Graphite-Encapsulated FeCo Nanoparticles Using A Hydrothermal Process. *Nanotechnology* 22, 375603.
- [7] A. Hossain, M. S. I. Sarker, M. K. R. Khan, F. A. Khan, M. Kamruzzaman and M. M. Rahman (2018), Structural, Magnetic, and Electrical Properties of Sol-Gel Derived Cobalt Ferrite Nanoparticles. *Appl. Phys. A* 124, 608:1-7.
- [8] M. Ma, Y. Wu, J. Zhou, Y. Sun, Y. Zhang and N. Gu (2004), Size Dependence of Specific Power Absorption of Fe_3O_4 Particles in AC Magnetic Field. *J. Magn. Magn. Mater.* 268, 33-39.
- [9] K. Zehani, R. Bez, E. K. Hlil et al. (2014), Structural, Magnetic, and Electronic Properties of High Moment FeCo Nanoparticles. *J. Alloys and Comp.* 591, 58-64.
- [10] J. M. MacLaren, T. C. Schulthess, W. H. Butler, R. Sutton, and M. McHenry (1999), Electronic Structure, Exchange Interactions, and Curie Temperature of FeCo. *J. Applied Physics* 85, 4833-4835.
- [11] S. J. Clark, M. D. Segal, M. J. Probert, C. J. Pickard, P. J. Hasnip and M. C. Payne (2005), First Principles Methods Using CASTEP. *Z. Kristallor.* 220, 567-570.
- [12] M. D. Segal, P. J. D. Lindan, M. J. Probert, C. J. Pickard, P. J. Hasnip, S. J. Clark and M. C. Payne (2002), First-Principles Simulation: Ideas, Illustrations and the CASTEP Code. *J. Phys.: Condens. Matter* 14, 2717-2744.
- [13] M. C. Payne, M.P. Teter, D. C. Allan, T. A. Arias and J. D. Joannopoulos (1992), Iterative Minimization Techniques for Ab Initio Total-Energy Calculations: Molecular Dynamics and Conjugate Gradients. *Rev. Mod. Phys.* 64, 1045-1097.
- [14] D. Vanderbilt (1990), Soft Self-Consistent Pseudopotentials in a Generalized Eigenvalue Formalism. *Phys. Rev. B* 41, 7892-7895.
- [15] T. H. Fisher and J. Almolf (1992), General Methods for Geometry and Wave Function Optimization. *J. Phys. Chem.* 96, 9768-9774.
- [16] H. J. Monkhorst and J. D. Pack (1976), Special Points for Brillouin-Zone Integrations. *Phys. Rev. B* 13, 5188-5192.
- [17] J. P. Perdew, K. Bruke and M. Ernzerhof (1996), Generalized Gradient Approximation Made Simple. *Phys. Rev. Lett.* 77, 3865-3868.
- [18] P. Y. Yu and M. Cardona, *Fundamentals of Semiconductors*; Springer-Verlag: Berlin (1996).
- [19] R. M. Dickson and L. A. Lyon (2000), Unidirectional Plasmon Propagation in Metallic Nanowires. *J. Phys. Chem. B* 104, 6095-6098.
- [20] P. M. Oppeneer, T. Maurer, J. Sticht, and J. Kibler (1992), Ab Initio Calculated Magneto-Optical Kerr Effect of Ferromagnetic Metals: Fe and Ni. *Phys. Rev. B* 45, 10924-10933.